

PRELIMINARY PERFORMANCE ANALYSES OF THE CONSTELLATION PROGRAM ARES I CREW LAUNCH VEHICLE

Mark Phillips, John Hanson, Terri Schmitt, Greg Dukeman, Jim Hays
NASA Marshall Space Flight Center, MSFC, AL 35812

Ashley Hill
Dynamic Concepts, Inc (DCI), Huntsville, AL 35812

Jessica Garcia
International Space Systems, Inc (ISSI), Huntsville, AL 35812

By the time NASA's Exploration Systems Architecture Study (ESAS) report had been released to the public in December 2005, engineers at NASA's Marshall Space Flight Center had already initiated the first of a series of detailed design analysis cycles (DACs) for the Constellation Program Crew Launch Vehicle (CLV) now known as ARES I. As a major component of the Constellation Architecture, the ARES I's initial role will be to deliver crew and cargo aboard the newly conceived Crew Exploration Vehicle (CEV), Orion, to a staging orbit for eventual rendezvous with the International Space Station (ISS). However, the long-term goal and design focus of the ARES I will be to provide launch services for a crewed Orion in support of lunar exploration missions. Key to the success of the ARES I design effort and an integral part of each DAC is a detailed performance analysis tailored to assess nominal and dispersed performance of the vehicle and to determine performance sensitivities. Results of these analyses provide valuable information to the program for the current design as well as feedback to engineers on how to adjust the current design in order to maintain program performance goals. This paper presents a subset of the ARES I performance analyses performed during the ARES I DAC-1 cycle. Deterministic studies include development of the ARES I DAC-1 reference trajectories, identification of vehicle stage impact footprints, an assessment of launch window impacts to payload performance, and the computation of select ARES I payload sensitivities. The dispersion write-up includes a description of the motivation for the dispersion work, the discipline customers for the results, the parameters varied, design variations versus flight day uncertainties, ground-rules, comparisons by month, choices of missions and vehicle models to run, and the latest results.

INTRODUCTION

Preliminary design of space vehicles typically relies on simple models in order to facilitate performance estimates as well as for high-level system trades of candidate configurations. Such models may be analytical, empirical (such as those derived through linear regression), or a composite. Inputs to such models are also typically of low fidelity. While such models are expedient in identifying initial vehicle configuration properties, experience suggests the addition of some amount (usually 15%-30%) of added mass margin to the final configuration to cover for model uncertainty and mass growth allowance. This added margin provides a means to preserve vehicle performance as additional constraints not considered in the initial design or as higher fidelity analyses bring more reality into the design. To identify

such additional constraint considerations, successions of design analysis cycles (DACs) are performed to validate the design or identify improperly sized components and predict corrective measures. At the close of each DAC a new configuration based on these corrections replaces the old thus maturing the vehicle design with each cycle. If all goes as planned, mass margins are not exceeded and expected performance is uncompromised.

By the time NASA's Exploration Systems Architecture Study (ESAS) report was released to the public in December 2005, engineers at NASA's Marshall Space Flight Center had already initiated the first of a series of detailed design analysis cycles (DACs) for the Constellation Program Crew Launch Vehicle (CLV) now known as ARES I. By the close of 2006, an additional two cycles had been performed with primary focus on driving out potential performance issues and identifying and documenting system requirements.

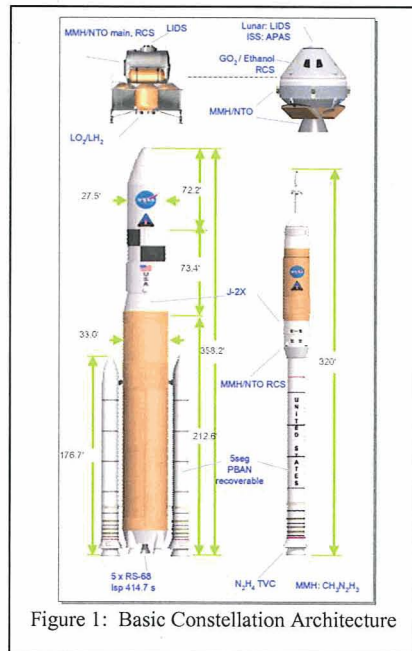


Figure 1: Basic Constellation Architecture

As a major component of the Constellation Architecture, the ARES I's initial role will be to deliver crew and cargo aboard the newly conceived Crew Exploration Vehicle (CEV), Orion, to a staging orbit for eventual rendezvous with the International Space Station (ISS). In this capacity, the ARES I and Orion will serve as a replacement for the aging space shuttle system. However, the long-term goal and design focus of the ARES I will be to provide launch services for a crewed Orion in support of lunar exploration missions. Key to the success of the ARES I design effort and an integral part of each DAC is a detailed set of performance analyses tailored to assess nominal and dispersed performance of the vehicle and to determine performance sensitivities. Results of these analyses provide valuable information to the program for the current design as well as feedback to engineers on how to adjust the current design in order to maintain program performance goals while maintaining minimum impact to cost and schedule. This paper presents a subset of the ARES I performance analyses performed during the ARES I DAC-1 cycle. Deterministic studies include development of the ARES I DAC-1 reference trajectories, identification of vehicle stage impact footprints, an assessment of launch window impacts to payload performance, and the computation of select

ARES I payload performance sensitivities. The dispersion write-up includes a description of the motivation for the dispersion work, the discipline customers for the results, the parameters varied, design variations versus flight day uncertainties, ground-rules, comparisons by month, choices of missions and vehicle models to run, and the latest results. A short discussion of the results and ramifications of each study are also provided.

DETERMINISTIC ANALYSES

Analyses of 3 Degree of Freedom trajectories serve a multi-functional purpose in the development of a space vehicle. For example, such trajectories can be used to affirm the vehicle concept, provide a reference or basis for higher fidelity system analyses (dispersion analyses, structural loads analysis, aero-thermal loads analysis, etc.), provide quick-action insight into performance measures leading to early design decisions (e.g. insertion altitude versus aero-thermal effects), aid in defining optimized operational use of the vehicle for specific scenarios (e.g. launch window effects or seasonal effects such as temperature or winds), provide visibility into how key design parameters behave during flight, isolate regions of flight that may require greater levels of scrutiny (e.g. start-up/shut-down transients, stage separations, coast phases, etc.), and identify aspects of the vehicle that more or less affect payload performance or other design considerations such as structural or thermal loads. All of these uses, however, depend on a credible vehicle concept, a solid set of guidelines and assumptions, and a well designed reference trajectory.

Reference Vehicle Configuration

As a result of NASA's ESAS, a two-launch vehicle architecture consisting of a medium-sized low earth orbit (LEO) access vehicle and a heavy lift cargo vehicle was selected (see Figure 1). The heavy lift cargo vehicle, or ARES V, would provide the majority of system logistics (Earth Departure Stage and Lunar Surface Access Module) for lunar missions while the medium-sized LEO vehicle, or ARES I, would be used for crew and light cargo delivery to prescribed LEO rendezvous targets for either lunar or ISS missions. The ARES I is configured as a two-stage plus payload vehicle with launch abort system (LAS) as shown in Figure 2. The LAS is similar to that used on Apollo but sized to meet Orion abort requirements. This configuration employs Shuttle and Saturn-derived propulsion systems and appears to offer low development and integration cost while maintaining component commonality with the ARES V. The current configuration features a 5-segment Shuttle RSRM-derived first stage and a Saturn-derived J-2X liquid oxygen (LOX) and hydrogen (H₂) engine for the second stage. Specific to the updated first stage booster is a new grain design tailored to produce acceptable peak levels in dynamic pressure. The J-2X engine, providing significantly higher thrust (293,750 lbf vs 230,000 lbf) and minimum Isp (448 sec vs 421 sec) than its Saturn J-2 predecessor, is sized to achieve overall payload performance. The fifth booster segment coupled with use of the J-2X also results in a reduction in upper stage propellant weight required (~80,000 lb less). The new configuration offers greater architectural commonality as the ARES V uses a 5-segment booster as part of its first stage and uses the same J-2X design for its upper stage. Information specific to this configuration as well as detailed guidelines and assumptions, propulsive characteristics (thrust, Isp, etc), aerodynamic data, and wind profiles used can be found in Reference XXX (not publicly available).

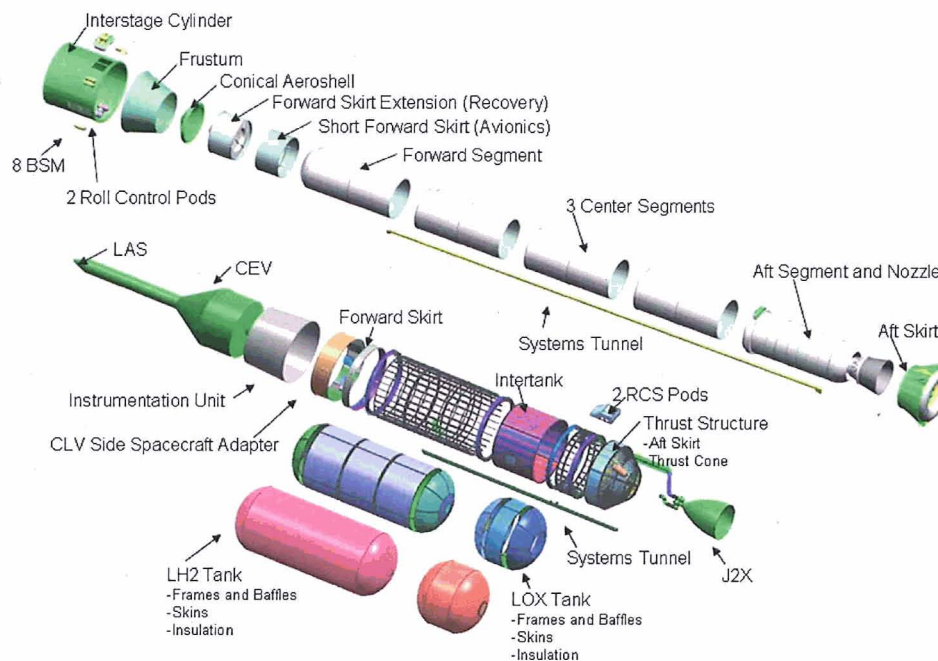


Figure 2: Design Analysis Cycle (DAC) 1 ARES I Reference Configuration

Mission Profiles

Figure 3 illustrates a typical mission profile for the ARES I. Due east launches and ISS missions share this same profile but not the same performance. The ascent phase begins when the launch countdown reaches zero at the opening or within the mission launch window. Approximately ¼ second (time $T=0.25s$) after first stage ignition, accumulated thrust is sufficient to lift the vehicle, hold-down restraints are released, and the vehicle begins to ascend vertically off of the pad. Upon clearing the tower (350 ft @ $T+6s$), the vehicle rolls to the prescribed mission flight azimuth and initiates an open loop steering (Roll, Yaw, Pitch) profile designed preflight for use during the atmospheric portion of flight. This steering profile

reflects predicted guidance commands necessary to meet trajectory design load constraints (e.g., dynamic pressure, Q ; angle of attack load, $Q\alpha$; side-slip load, $Q\beta$; etc.) and engine cutoff conditions (radius, velocity, flight path angle, and orbit plane) while optimizing payload performance. For nominal flight conditions, this profile initiates an aerodynamic angle ramp-down at $\sim T+16s$ ($Q=150$ psf) to initiate gravity turn flight at $\sim T+21s$ (gravity turn flight provides the lowest aerodynamic load environment for the vehicle during atmospheric flight). This flight mode is continued through the point of maximum dynamic pressure (max- Q , $\sim T+59s$) and through reducing dynamic pressure until the thrust from the SRB has diminished to a sufficiently low enough level ($\sim 40,000$ lb) to permit first stage separation at $\sim T+127s$. At this time stage separation is initiated and the vehicle coasts for approximately 1 seconds ($\sim T+128s$) followed by the second stage J-2X start-up command. After ~ 5 seconds ($\sim T+133s$) the J-2X reaches 100% thrust and closed-loop guidance provides vehicle steering commands for the remainder of the second stage ascent profile. The command to jettison the LAS is issued 35 seconds after the J-2X start-up command was received. The vehicle then continues second stage ascent until the engine shutdown command is issued ($\sim T+557s$) and the main engine cut off condition (MECO) is attained ($\sim T+559$ s, altitude = 55 nmi, orbit = -30×100 nmi, inclination = 28.5 or 51.6 deg). Following development of the DAC-1 trajectory presented here, Orion heating analyses identified thermal issues with the DAC-1 MECO insertion altitude. Evidence justifying raising the altitude from 55 nm to 70 nm was presented and a follow-on study (not presented) ensued. As a result of that analysis, the MECO target to be used in the next DAC was changed (altitude = 70 nmi, orbit = -11×100 nmi, inclination = 28.5 or 51.6 deg). The change in perigee target resulted from the desire to maintain the upper stage impact area in the Indian Ocean.

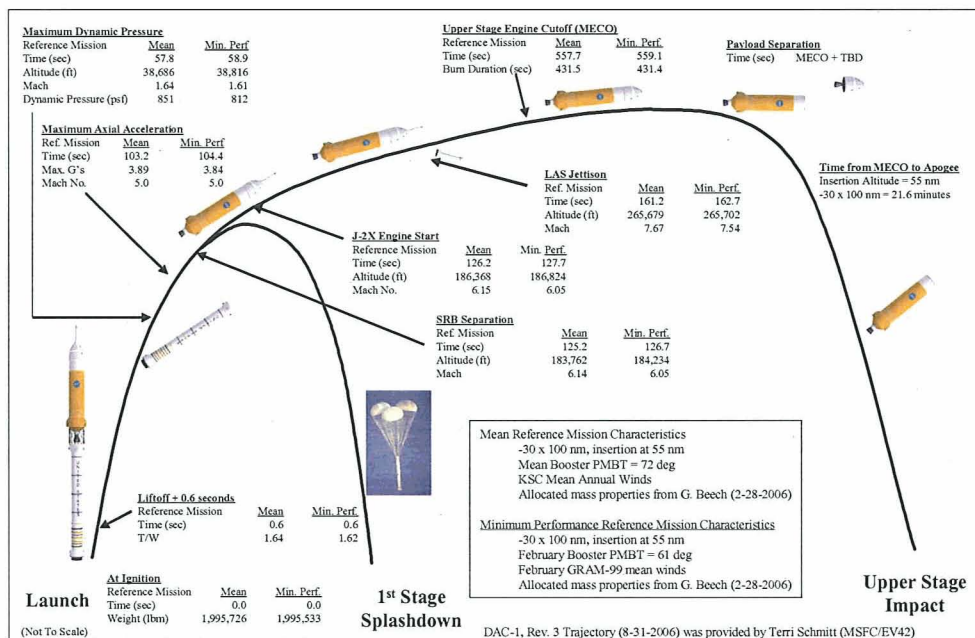


Figure 3 – Representative DAC-1 Rev 3 Trajectory Profile (Exploration Mission)

First Stage Entry Profile (Delete?)

The first stage entry profile begins at first stage separation ($\sim T+127s$). Prior to this time, separation and recovery systems appropriate to each vehicle element (first stage, inter-stage, and upper stage) are enabled and, at the appropriate times, commands are sent to these systems to perform the separation and recovery actions. The reentry profile of the 1st stage is modeled from stage separation until the stage reaches an altitude of 15,000 feet at which time the parachutes are deployed. Following separation, the booster typically follows a path as depicted in Figure 3. Upward momentum carries the booster to an apogee of approximately 240,000 ft. The booster then falls back into the atmosphere and into a recovery area approximately 150 nm down range from the launch site. A booster pitch maneuver immediately following separation is incorporated to assure that the booster will not re-contact the upper stage and that the booster attains an attitude commensurate with the desired SRB reentry profile. This profile is based on the STS SRB reentry described in Reference 3 [document SE-019-053-2H (entry angle of attack ranges

provided by Bruce McWhorter / ATK Thiokol]]. To model trajectory behavior, angle of attack profiles versus altitude were generated using this data and are shown in Table 1. These profiles are used to determine the first stage entry trajectories and associated entry footprints (recovery areas) for each design reference mission.

Table 1: SRB Reentry - Angle of Attack Profiles

<i>SRB Angle of Attack Profiles</i>		
Altitude (feet)	Angle of Attack (degrees)	
	Minimum Drag	Maximum Drag
20,000	113	97
30,000	158	152
50,000	167	158
100,000	150	130
150,000	119	106
300,000	119	106

Reference Trajectory Performance

Development of a good reference trajectory set is essential to proper analysis of a given vehicle configuration. For DAC-1 it was decided that two reference trajectories for each mission would be used to support minimum performance and other downstream trajectory analyses. For minimum performance analysis, a February Propellant Mean Bulk Temperature (PMBT) of 61° F and February GRAM-99 mean monthly winds would be used to derive payload performance. All other trajectory analyses (US entry, launch window, vehicle sensitivity, etc.) would use a mean booster PMBT of 72° F and mean annual winds. To support GN&C dispersion studies, design input trajectories tailored to specific analysis goals (e.g., maximum load, August PMBT=82° F, etc.) were provided.

For DAC-1, two different upper stage thrust values were used depending on mission. The lunar exploration mission used a vacuum thrust on the J-2X upper stage engine at 293,750 pounds-force (lbf) and the ISS mission used the 273,750-lbf thrust value from the previous analysis cycle. Mass properties for the DAC-1 configuration are provided in Table 2. Detailed aerodynamic data and booster thrust table were too detailed to be included with this paper but may be found in Reference xx.

Table 2: ARES I DAC-1 Rev. 3 Mass Properties (all weights in lb)

First Stage		1,598,715
	Stage Inert Weight	225,197
	Loaded Propellant	1,373,518
Interstage		7,688
	Inter-stage Dry Mass	6,104
	Expendables	1,584
Second Stage		317,659
	Stage Dry Mass	26,445
	Engine	5,360
	Unusable Residuals	2,122
	Pressurized Gases	1,185
	Ascent Propellant *	279,825
	Flight Performance Reserve (FPR) *	2,146
	Fuel Bias	374
	MPS Engine Purge Helium	115
	RCS Propellants	88
Launch Abort System		13,228
Mass at Ignition (WITHOUT Payload)		1,937,290
Notes:		
* Ascent propellant and FPR for the Exploration mission reference trajectories on 8/23/06.		
The total usable propellant (ascent + FPR + fuel bias) = 282,345 lb.		

Payload performance was optimized using the Program to Optimize Simulated Trajectories (POST) program. The target orbit for the Exploration and ISS missions was -30 x 100 nm, with the insertion altitude at 55 nm. Target inclination and upper stage thrust level were changed based on the particular mission flown (Exploration: 28.5°, 293750 lbf; ISS: 51.6°, 273,750 lbf). Summaries, detailing both the performance and selected trajectory parameters, are shown in Table 3. Performance predictions for each reference trajectory include accounting for payload adapter and ascent performance margin.

Table 3: Rev. 3 Trajectory Summaries

Trajectory Description	Rev. 3-M	Rev. 3-M	Rev. 3-Min. Perf.	Rev. 3-Min. Perf.
Trajectory Date	8/31/2006	8/31/2006	8/31/2006	8/31/2006
Mission Description	Exploration	ISS	Exploration	ISS
Winds	KSC Mean Annual	KSC Mean Annual	February GRAM-99	February GRAM-99
Booster PMBT (deg F)	72	72	61	61
Booster Designation	RSRMV16606- TRDG	RSRMV16606- TRDG	RSRMV16606- TRDG	RSRMV16606- TRDG
US Engine Thrust (lbf)	293,750	273,750	293,750	273,750
Mass Properties	Allocated	Allocated	Allocated	Allocated
Summary				
Gross wt at SRB ignition (lb)	1,995,726	1,989,843	1,995,533	1,989,606
SRB loaded propellant	1,373,518	1,373,518	1,373,518	1,373,518
SRB inert weight	225,197	225,197	225,197	225,197
Interstage	7,688	7,688	7,688	7,688
Upper Stage usable ascent propellant	279,822	279,905	279,825	279,909
Launch Abort System	13,228	13,228	13,228	13,228
Injected Weight	96,273	90,307	96,076	90,066
Usable Propellant Reserve	2,149	2,066	2,146	2,062
Usable fuel bias LH2	374	374	374	374
Residual propellant	2,122	2,122	2,122	2,122
MPS helium purge	115	115	115	115
Pressurant gases	1,185	1,185	1,185	1,185
Dry weight (w/ot engine)	26,445	26,445	26,445	26,445
Engine Weight	5,360	5,360	5,360	5,360
RCS propellant & residuals	88	88	88	88
Injected Payload Weight to delivery orbit (lb)	58,435	52,552	58,242	52,315
Injected Payload Wt to delivery orbit (mt)	26.51	23.84	26.42	23.73
Integrated Vehicle Allowance	1,650	1,650	1,650	1,650
Gross Payload to orbit (lb)	56,785	50,902	56,592	50,665
Ascent Performance Margin	7,877	7,877	7,877	7,877
Net Payload to delivery orbit (inc. adapter) (lb)	48,908	43,025	48,715	42,788
Spacecraft Adapter (payload chargeable) (lb)	1,300	1,300	1,300	1,300
Net Payload to delivery orbit (w/out adapter) (lb)	47,608	41,725	47,415	41,488
Net Payload to orbit (mt)	21.59	18.93	21.51	18.82
Trajectory Parameters				
Launch azimuth (deg)	88.9	49.8	87.8	50.0
Total burn time (sec)	557.7	588.9	559.1	590.5
Total ascent ideal ΔV (fps)	29,576	30,326	29,594	30,354
Maximum acceleration (g's)	3.89	3.93	3.84	3.88
Time at Max. acceleration (sec)	103.2	103.2	104.4	104.4
Time at Max. Q (sec)	57.8	56.9	58.9	57.5
Maximum Dyn. Pressure (psf)	851	848	812	812
Mach Number at Max. Q	1.64	1.62	1.61	1.57
Altitude at Max. Q (ft)	38,686	38,103	38,816	37,743
SRB jettison time (sec)	125.2	125.2	126.7	126.7
SRB jettison altitude (ft)	183,762	191,491	184,234	192,199
SRB jettison Mach Number	6.14	6.21	6.05	6.11
SRB relative fpa (deg)	23.81	25.66	24.08	26.00
LAS jettison time (sec)	161.2	161.2	162.7	162.7
LAS jettison altitude (ft)	265,679	279,934	265,702	280,266

Upper Stage Entry Trajectory

The mission profile for the upper stage essentially follows the ascent profile to the nominal MECO conditions, through payload separation and apogee (100 nmi), and then reentering and breaking apart in the Earth's atmosphere (reference Figure 2) while on the return path toward perigee (-30 nmi). **The upper stage and adapter reenter the atmosphere as an integral unit.**

To properly analyze the entry profile of the upper stage, the variation in two factors, stage orientation and atmospheric density, is accounted for. Due to lack of control, the orientation of the upper stage may vary during reentry. To model this behavior, three sets of drag coefficients (side-entry, end-entry, and tumbling) are used to define the entry footprint for each design reference mission. When the stage reenters on its side (angle of attack = 90°), the drag causes it to impact quicker. With an end entry (angle of attack = 0°), the impact location is further downrange. A tumbling reentry results in an intermediate impact distance.

To account for variability in atmospheric conditions and variations resulting from ascent dispersions, trajectories are generated using the above drag coefficients with the atmospheric density varied by $\pm 30\%$. This is an early estimate that will be superseded by results of Monte Carlo dispersion simulations. Coupled with orientation effects, the resulting shortest downrange distance is represented by a denser atmosphere and a side-entry orientation while the furthest impact location is represented by a less dense atmosphere and an end-entry orientation. **Note to Mark: We need to de-emphasize the 30% variation because I just heard the overall variation is more like 2%.** In the absence of a detailed debris model and high fidelity dispersion simulation, breakup of the upper stage was modeled using a footprint with the same dimensions as the dispersed STS-51D External Tank (ET) impact footprint. For this model, the footprint toe is located 439 nm downrange of the nominal impact point, the footprint heel is located 554 nm up-range of the nominal impact point, and the maximum footprint width (located at the nominal impact point) is 36.6 nm. This footprint model is illustrated in Figure 4.

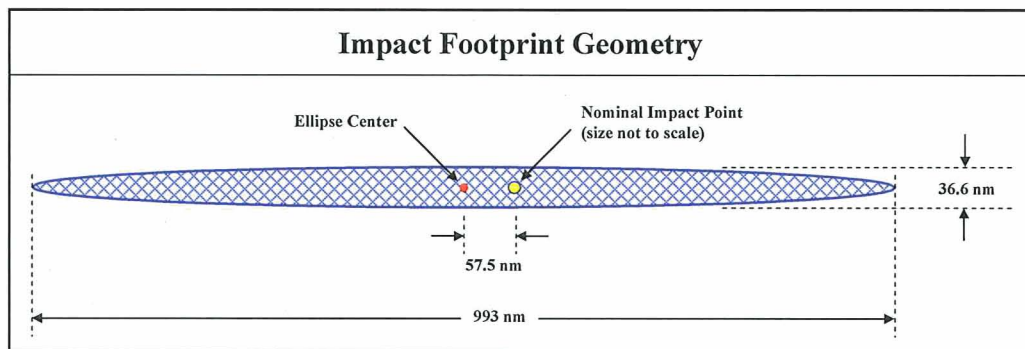


Figure 4: ARES I Upper Stage Impact Footprint Geometry

Overlays of this model onto the up-range and down-range impact points defined by the orientation and density models can then be used to locate the overall upper stage footprint for a given set of MECO conditions.

A representative upper stage footprint from a trade study performed in November 2005 (Reference 4) is shown in Figure 5. As a consequence of that study, insertion target conditions were changed from a 30x160 nm orbit inserted at 57 nm to a -30x100 nm orbit inserted at 55 nm. This change improved overall payload performance for the Orion at the rendezvous orbit and provided desired containment of the upper stage debris footprint within an unpopulated region in the Indian Ocean (Figure 6). This activity is performed as a normal part of each DAC to verify that the implementation of any vehicle performance updates do not result in the footprint encroaching on populated areas.

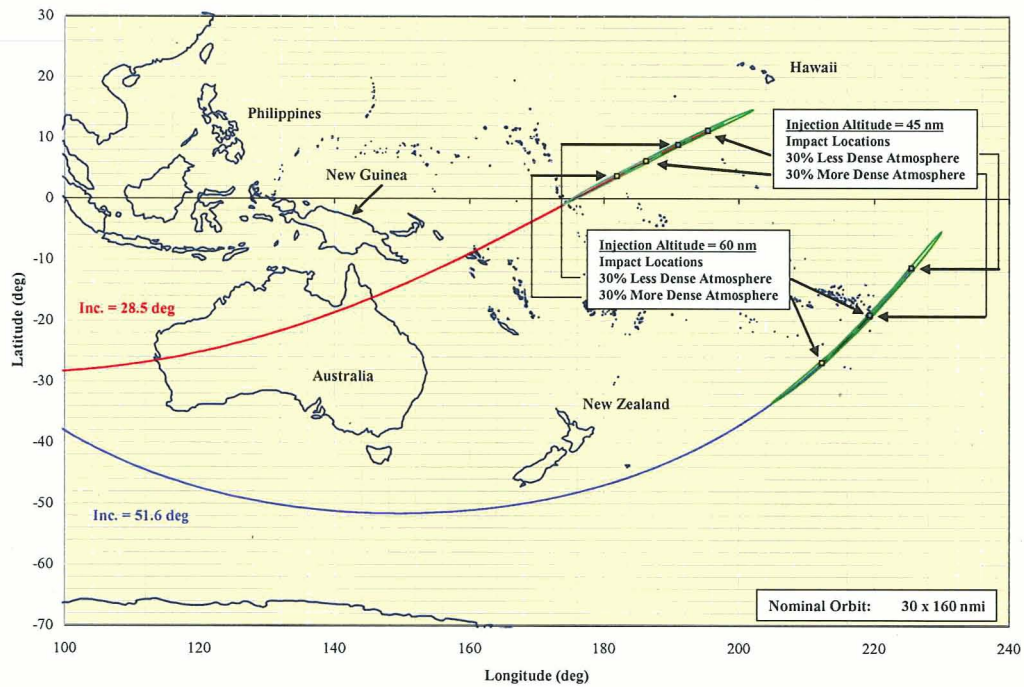


Figure 5: Upper Stage Impact Zones for 30x160 nm Orbit

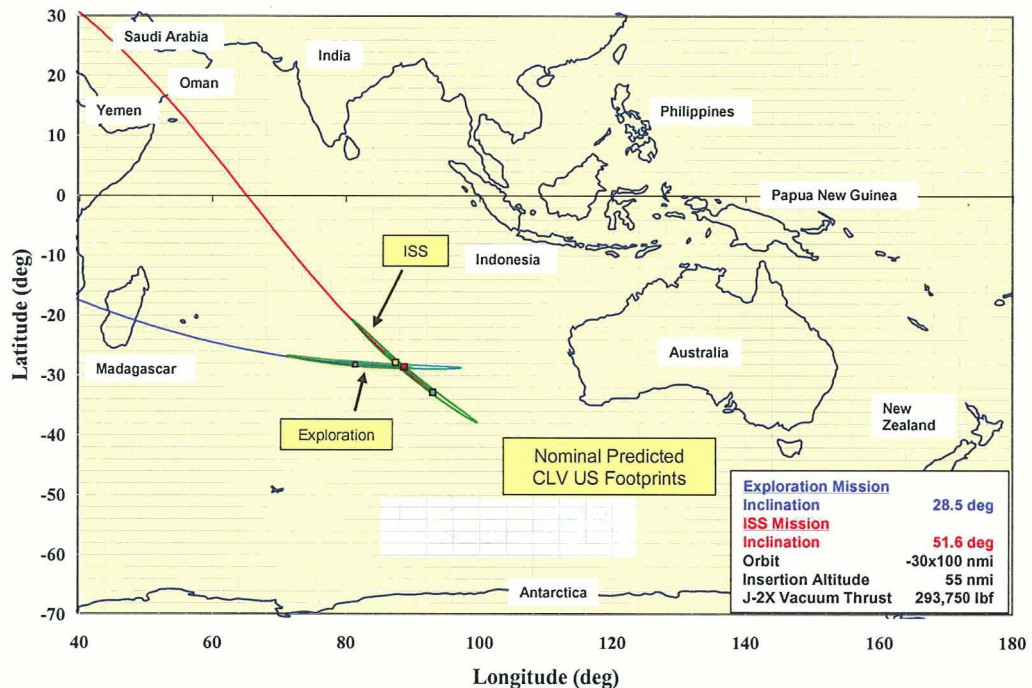


Figure 6: Upper Stage Impact Zones for -30x100 nm Orbit at 55 nm Insertion Altitude

Launch Window Effects

By definition, both the Exploration and ISS missions are to be designed as rendezvous missions. To facilitate Exploration missions, the launch of the ARES I must be constrained to inject the Orion into an orbit such that LEO rendezvous with a previously launched EDS/LSAM is possible. Similarly, for ISS

missions, launch of the ARES I must be constrained to permit rendezvous with an orbiting ISS. To provide sufficient launch opportunity while adhering to rendezvous constraints, some degree of steering capability is required. However, the capability to steer the vehicle during ascent comes at some cost to payload performance. Such losses can be predicted and can be accounted for by setting aside a portion of flight performance margin to cover the predicted loss. While this results in sub-optimal payload performance, launch opportunity and rendezvous constraints can be accommodated. The primary trade is between launch window duration and payload loss. In general, increases in launch window durations produce greater payload losses. However, the cost for some missions is more expensive than others in terms of payload penalty. For specified window duration, injections into lower orbital inclinations produce less payload penalty. Likewise, for a fixed payload penalty, injections into lower orbital inclinations produce larger launch windows. The Constellation program satisfies launch opportunity by defining launch window duration by mission. For Exploration missions, sufficient flight performance margin must be set aside to support a 90-minute launch window without compromising required mission payload performance. For ISS missions, margin set-aside to support a 10-minute launch window is required for ISS payloads. Changes to the vehicle that alter ascent performance will affect predicted payload loss associated with these launch window requirements. As part of each DAC, the penalty for providing these windows is assessed. Figure 7 illustrates the payload impact as a function of launch time offset. From this figure, sensitivity to launch time offset is noticeably greater for ISS missions than for Exploration missions. This is expected due to the lower inclination of the Exploration mission. Also of particular note is the lack of symmetry about the nominal launch time for the lower inclination. This is due in part to the effects of launch azimuth and subsequent yaw steering characteristics necessary to converge to the proper orbit inclination and descending node target. The noticeable double-hump feature for the lower inclination (28.5 deg) is due mostly to the reference trajectory not employing upper stage yaw steering during payload optimization (yaw steering was permitted for all other launch times) and the launch site passing through the target plane twice in quick succession. Figure 7 also provides the means to identify mission launch time offsets for a particular launch window performance allocation or identify payload penalty for specified window duration. Figure 8 illustrates results for the latter; identifying a ~300 lb payload impact to Exploration mission performance in order to achieve a 90-minute window and a ~635 lb payload impact to ISS mission performance in order to maintain a 10-minute window. For DAC-1, the vehicle configuration resulted in the Exploration mission exceeding its launch window allocation (of 260 lb) by 40 lb, thus necessitating an update to that allocation.

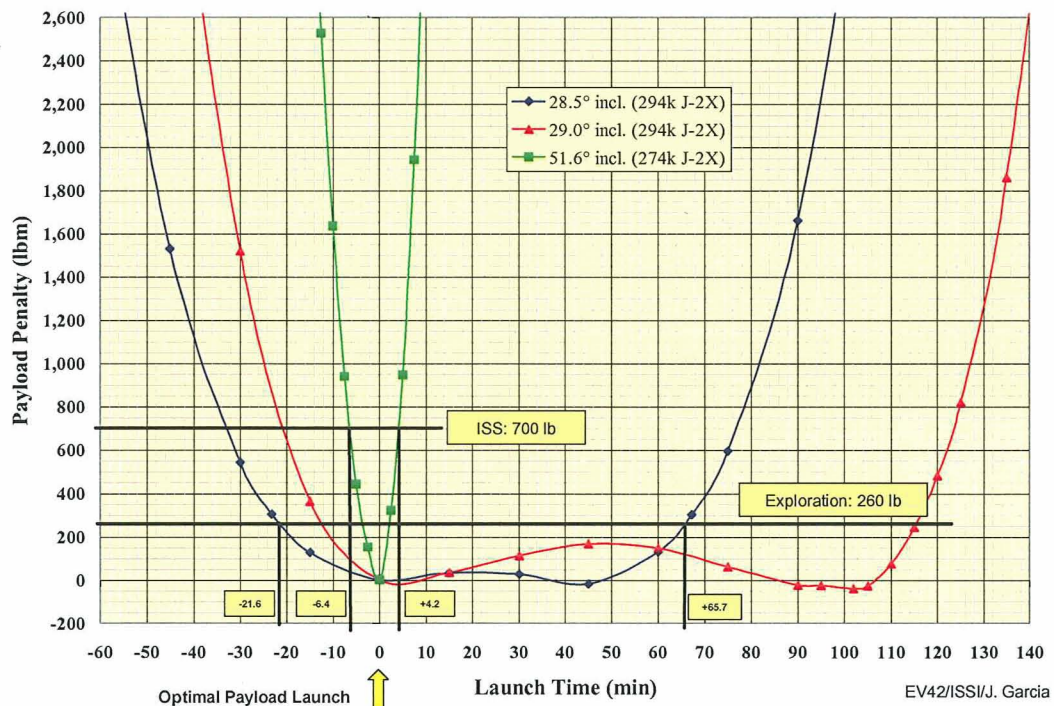


Figure 7: DAC-1 Rev3 Payload Penalty Vs Launch Time Offset

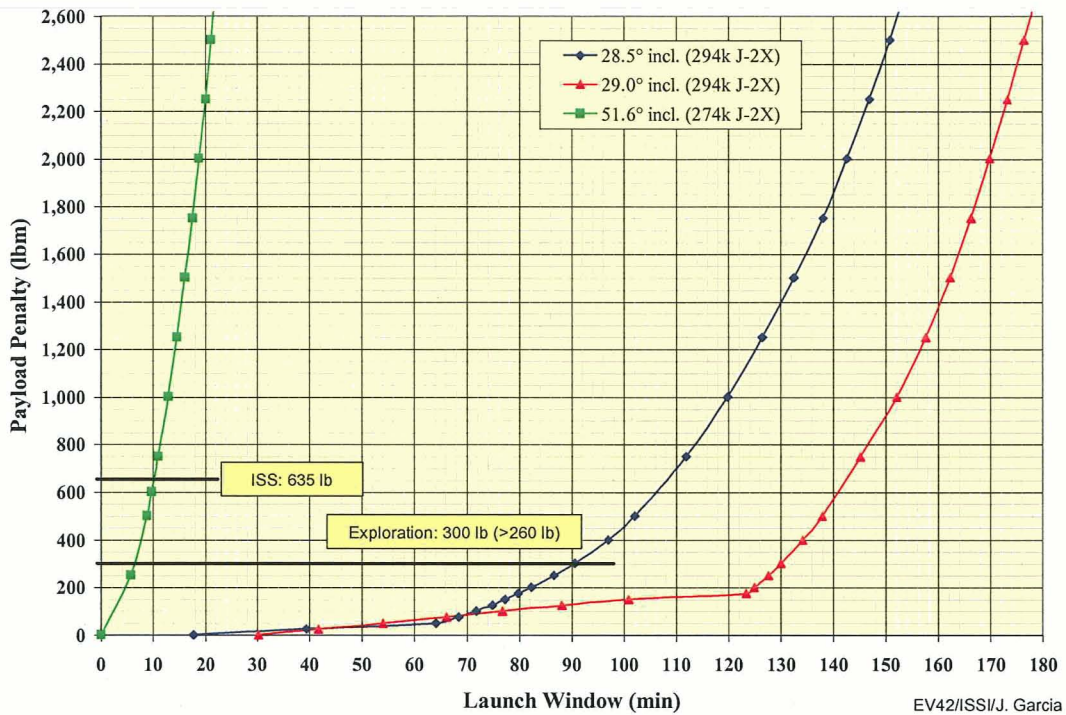


Figure 8: DAC-1 Rev3 Payload Penalty Vs Launch Window Duration

Vehicle Performance Sensitivities

The effects of different design parameters on delivered payload are investigated for each DAC vehicle configuration. This analysis reveals the impact of off-design conditions on the delivered payload and can identify potential design concentration areas if significant improvements in payload performance are sought. To determine a given sensitivity, payload performance resulting from a change in a specific design parameter is compared to that delivered by the reference trajectory. The change in payload performance per change in parameter defines the given sensitivity. Payload performance was re-optimized for each change. The DAC-1 Rev. 3-Mean trajectory was used as the basis for identifying these sensitivities.

Design parameters studied for each vehicle configuration are grouped into six categories: Upper Stage, Launch Abort System, Inter-stage, RSRM first stage, Aerodynamic, and Mission Design. For all cases, only payload performance sensitivities for trajectories reaching nominal MECO conditions are evaluated. Sensitivities for other flight scenarios, such as abort situations, are not yet part of this analysis. A summary of the parametric changes within each category and their associated payload performance sensitivities are provided in [Table 4](#) through [Table 9](#). Most of the effects are linear, but a few are not (e.g. LAS jettison time). Thus, re-optimization of the vehicle trajectory should be performed to validate any sensitivity-based performance predictions.

Vehicle Performance Sensitivities: Upper Stage Sensitivities

The effects of changing various Upper Stage parameters were analyzed with particular parameters studied reflecting changes in propulsion system performance and mass properties. Propulsive sensitivities are based on a ± 1 -second change in engine Isp and a $\pm 10\%$ change in available thrust. Mass property sensitivities are based on a $\pm 10,000$ lb change in available Upper Stage propellant and were calculated for two cases. For the first mass property case, propellant is added or subtracted with no corresponding change in stage structural mass. For the second mass property case, propellant is added or subtracted but with constant stage mass fraction (w/o engine weight) as a constraint. The results are shown in [Table 4](#).

Table 4: DAC-1 Rev3 Upper Stage Sensitivities

Sensitivity	Exploration Mission Tvac=294klb	ISS Mission Tvac=274klb	Units
J-2X Isp	290	268	lb of payload / second change in J-2X Isp
J-2X Thrust	3,033	3,327	lb of payload / 10% change in J-2X thrust
Upper Stage Propellant Loading (no change in dry weight)	92	68	lb of payload / 1,000 lb change of US propellant
Decrease Upper Stage Propellant Loading by 10,000 lb (recalculate the dry weight)	-66	184	lb of payload
Increase Upper Stage Propellant Loading by 10,000 lb (recalculate the dry weight)	-87	-325	lb of payload

Analysis results show that increases in Isp and thrust as well as increases only in propellant load produce payload performance gains. The latter (increase in propellant), however, does not account for any structural growth of the upper stage necessary to accommodate the increased propellant. To more realistically predict how propellant changes affect payload, estimates of the structural growth are included by assuming that the mass fraction essentially remains constant for small changes. Of particular interest is the increase in ISS payload capability resulting from a reduction in propellant load and corresponding decrease in upper stage mass. This is a residual effect of the ARES I propellant load being optimized for the Exploration mission as well as for an earlier vehicle configuration (DAC-0) and maintaining that load across configuration updates. Of additional note is the respective level of propellant load sensitivity for the Exploration mission versus the ISS mission with the latter showing greater sensitivity. The ISS mission also exhibits greater sensitivity when structural changes are accounted for.

Vehicle Performance Sensitivities: LAS Sensitivities

Performance sensitivities for the LAS are based only on mass property changes for that system (mission design sensitivities are covered below). Mass sensitivities analyzed include a $\pm 1,000$ lb change in LAS system weight and an assessment of impact to payload from carrying the system from launch to orbit injection. Results are shown in Table 5. Results are unsurprising. An increase in the LAS system weight negatively influences payload performance. Carrying the LAS to orbit is also shown to be prohibitively expensive in terms of payload capability loss (~20% nominal payload capability).

Table 5: DAC-1 Rev3 LAS Mass Sensitivities

Sensitivity	Exploration Mission Tvac=294klb	ISS Mission Tvac=274klb	Units
LAS Jettison Weight	-124	-120	lb of payload / 1,000 lb increase in LAS Weight
No LAS Jettison	-11,554	-11,624	lb of payload

Vehicle Performance Sensitivities: Inter-Stage Sensitivities

Performance sensitivities for the Inter-stage are also based only on mass property changes for that system. Mass sensitivities analyzed include a $\pm 1,000$ lb change in Inter-stage system. Results are shown in Table 6 and indicate that an increase in the inter-stage system weight negatively influences payload performance.

Table 6: DAC-1 Rev3 Inter-Stage Mass Sensitivities

Sensitivity	Exploration Mission Tvac=294klb	ISS Mission Tvac=274klb	Units
Interstage Weight	-103	-100	lb of payload / 1,000 lb increase in the Interstage Weight

Vehicle Performance Sensitivities: First Stage Sensitivities

As with the Upper Stage, First Stage sensitivities studied reflect changes in propulsion system performance and mass properties. Propulsive sensitivities are based on a ± 1 -percent change in booster thrust and a ± 1 degree change in propellant mean bulk temperature (PMBT). PMBT changes have a direct relationship to the burn rate of the motor. For example, a 4° F change is equivalent to a 1 mill (0.001 inches) change in burn rate. Mass property sensitivities are based on a $\pm 1,000$ lb inert stage weight and a $\pm 1,000$ lb change in available First Stage propellant while holding the Isp curve constant. The results are shown in Table 7.

Table 7: DAC-1 Rev3 First Stage Sensitivities

Sensitivity	Exploration Mission Tvac=294klb	ISS Mission Tvac=274klb	Units
SRB Jettison Weight	-103	-100	lb of payload / 1,000 lb increase in the SRB jettison weight
SRB Thrust	1,181	1,130	lb of payload / 1% change in SRB thrust
SRB PMBT	40	40	lb of payload / 1 deg change in SRB PMBT
SRB Propellant (assume constant Isp)	50	50	lb of payload / 1,000 lb change in SRB propellant (constant Isp)

Following the same trend as the inter-stage, weight changes have an opposite effect on the delivered payload. Increases in inert weight result in decreased payload at orbital injection. The increased PMBT values will increase the payload slightly. Average variation over the year ranges from $\sim 60^\circ$ F to $\sim 82^\circ$ F or about 22 degrees. While this effect can dramatically increase payload (~ 800 lb), it also has impacts on other trajectory parameters, such as increasing the maximum dynamic pressure and axial acceleration. Changing the first stage thrust level has the greatest impact on the payload performance of the vehicle.

Vehicle Performance Sensitivities: Aerodynamic Sensitivities

The effects of changing aerodynamic parameters were also investigated. Parameters studied were a ± 10 percent change in reference area and a ± 10 percent change in base force. The latter also provides a sensitivity estimate for changes in axial force coefficient. Results are shown in Table 8.

Table 8: DAC-1 Rev3 Aerodynamic Sensitivities

Sensitivity	Exploration Mission Tvac=294klb	ISS Mission Tvac=274klb	Units
Aerodynamic Reference Area	-34	-31	lb of payload / 1% change in reference area
Base Force	-1	-1	lb of payload / 10% change in base force magnitude

Results indicate that base force changes essentially have no adverse effect on payload performance; however, changes in the reference area, if large, will have a significant effect. Reducing either parameter results in payload increase.

Vehicle Performance Sensitivities: Mission Design Sensitivities

The last sensitivity category reflects how vehicle performance is affected by changes in mission design parameters. Effects studied include stage separation time, upper stage coast time, LAS jettison time, target orbit inclination, monthly variation in PMBT and wind profile, upper stage engine selection (294klb vs. 274klb), and maximum dynamic pressure constraints. For highly non-linear effects, multiple change levels are provided where appropriate to more clearly characterize the effect. For remaining effects, the average sensitivity is provided. The baseline trajectories are the Rev. 3-M trajectories listed in Table 3. Results are shown in Table 9 and are briefly discussed in the following paragraph.

Analysis of event time sensitivities indicates greater sensitivity to separation time and coast time than for LAS jettison time. However, this observation only applies to changes on the order of a few seconds. Practically, separation and coast times will not change appreciably from the nominal time as such changes will be driven by separation sequence and upper stage startup requirements. The effect of the LAS jettison is not easily dismissed as abort requirements could require significant delay in jettison time thus producing effects similar to separation and coast time. Inclination effects are of the same order with greater sensitivity at the higher inclination. The trend is clear with higher inclinations producing less performance. The effect of changing inclination from the Exploration Mission to the ISS Mission for each thrust level is also provided. Temperature variations and wind profiles combine to provide a non-linear relationship. The warmer months give a slightly better performance as compared to the mean reference temperature and winds. However, higher PMBT also results in increased dynamic pressure and axial accelerations. Limits on the maximum dynamic pressure result in lofted trajectories. The greater the limit, the more loft is produced and the impact on the payload is more pronounced. The non-linear effect is also more pronounced. Of greatest interest is perhaps the effect of engine selection. The J-2X is expected to provide 294k lb thrust in support of Exploration missions. Near term development is expected to produce a lower thrust version which has been deemed adequate for supporting ISS missions (which will occur earlier per schedule). Should development not occur as planned or occur ahead of schedule, the effect on payload due to available thrust is of extreme interest. Results indicate that for the ISS, a ~2,200 lb payload gain is possible at the higher thrust level (early delivery and integration); while for the Exploration mission, if development fails to produce the expected thrust level, a ~2,200 lb loss in payload capability is possible. Recent developments though indicate that the higher thrust J-2X will be the standard for both the ISS and Exploration missions.

Table 9: DAC-1 Rev3 Mission Design Sensitivities

Sensitivity	Exploration Mission Tvac=294klb	ISS Mission Tvac=274klb	Units
SRB Separation Time	-107	-110	lb of payload / second change in the SRB separation time
US Coast Time	-132	-133	lb of payload / second change in coast time
LAS Jettison Time (average)	-9.5	-8.7	lb of payload / second change in LAS jettison time
1° change in inclination (29.5° and 52.6°, respectively)	-142	-186	lb of payload
2° change in inclination (30.5° and 53.6°, respectively)	-278	-374	lb of payload

Sensitivity	Exploration Mission Tvac=294klb	ISS Mission Tvac=274klb	Units
23.1° change in inclination (increase from 28.5° to 51.6°, J-2X thrust = 293,750 lbf)	-3,702	n/a	lb of payload
-23.1° change in inclination (decrease from 51.6° to 28.5°, J-2X thrust = 273,750 lbf)	n/a	3,641	lb of payload
February PMBT (61°) and Feb. GRAM-99 Winds	-193	-238	lb of payload
August PMBT (82°) and Aug. GRAM-99 Winds	76	183	lb of payload
J-2X Thrust change (from reference trajectories)	-2,242	2,181	lb of payload / 20,000 lbf change in J-2X thrust (ISS level to Expl. level)
Reduce Max. Q by 25 psf	-320	-338	lb of payload
Reduce Max. Q by 50 psf	-1,569	-1,671	lb of payload
Reduce Max. Q by 75 psf	-4,383	-4,740	lb of payload

MONTE CARLO DISPERSIONS

Motivation

The purpose of conducting Monte Carlo simulations is to determine the worst-case results for any discipline that drives vehicle design. The worst case payload performance, for example, might be driven by a cold first stage solid rocket combined with a low-performing J-2X engine. The worst case structural bending loads might be driven by a hot first stage and a significant headwind. Simply combining bad values of certain parameters and running a simulation can yield overall bad cases, but what is unknown is where these cases stand with respect to the overall distribution of all flights. In a Monte Carlo simulation, all the parameters of interest are varied randomly within their estimated uncertainty distributions in order to see what happens. By performing many independent randomly varied simulations, an overall distribution of the flight results (parameters of interest) is obtained. Individual parameter variations will also be conducted as part of the Ares-I vehicle design effort in order to understand the sensitivity to each parameter. Other methods of varying the parameters exist (references), but none have been identified so far that yield known statistics for the results and also are attractive for a large number of input parameters. This section lists the design discipline customers, discusses the Monte Carlo setup and input parameters varied, discusses the results as a function of launch month, lists the missions and months of interest for finding the worst case results, and shows the most recent 6 Degree of Freedom dispersion results.

Customers

Table 10 shows the current list of Ares-I dispersion customers. This list will most likely grow with time. Each customer is interested in finding the worst case trajectory parameters that impact their design. This worst case may be the actual worst result from the Monte Carlo runs, or it may be a 3-sigma case, for example, if the discipline in question is designing to a 3-sigma value.

Table 10. Current Dispersion Simulation Customers

Discipline Area	Current Use of Results
Aerothermal	Examines all trajectories to determine the worst case for aerothermal indicators at various body points. Also, for the crewed vehicle, examines worst cases for nominal and abort heating (for example, heating on the Service Module while it executes an abort burn). Examines aeroheating during stage re-entry.
Natural Environments	Examines results for understanding of the wind modeling, for purposes of ensuring the correct modeling for design
SRB Recovery	Uses all SRB separation state vectors as initialization for re-entry Monte Carlo simulations, for thermal and recovery system design
Structural Analysis	Uses worst case dynamic pressure times aerodynamic angle for determination of Ares-I ascent structural bending loads. Similar needs for Orion (crewed spacecraft) design
Venting	Looks for worst case for venting design; related to change in pressure but more complicated
Orion (crewed spacecraft) Abort	What are the worst case dispersions from which an abort may occur? Failure events combined with dispersed trajectories are part of this. Also, minimum time after abort before atmospheric entry; examination of abort modes (abort to orbit, etc.)
Abort Test Booster Design	What are the variations in launch vehicle flight that drive the design of the Abort Test Booster?
Reaction Control System Design	The variation of the vehicle acceleration vector direction with respect to the vehicle body centerline impacts RCS design
Flight Mechanics	Determination of Flight Performance Reserve (how much extra fuel is needed to ensure successful orbit injection?)
GN&C	Orbit insertion accuracy; upper stage impact zone
GN&C	Flight control analysis and specification of requirements on sensors and actuators
GN&C	Guidance analysis (determining the appropriate guidance approaches)
Acoustics	Examines standard trajectory output for acoustic design
Main Propulsion System (tanks, fuel lines)	Needs fuel inventory results and acceleration dispersions for MPS design
Liftoff analysis	Trajectory with lowest acceleration off the pad for liftoff drift. Trajectory with highest acceleration off the pad for umbilical removal.

Parameters Varied

Table 11 lists the parameters currently being varied. The modeling of each parameter is specified by the discipline or vehicle element providing the uncertainty estimates. Additional parameters will be added as appropriate during the design process.

Table 11: Parameters Varied

Parameter Area	Parameters Varied
SRB	Burn rate (Propellant Mean Bulk Temperature uncertainty is covered by the burn rate dispersion), loaded propellant, specific impulse, low-level thrust tailoff model, nozzle location, nozzle cant angle
J-2X	Mixture ratio, thrust, specific impulse, startup and shutdown transient thrust model, nozzle location, nozzle cant angle
Upper Stage	Liquid oxygen loaded, liquid hydrogen loaded
Aerodynamics	All aerodynamic force and moment coefficients and engine power-on base force
Atmosphere	Global Reference Atmosphere Model (reference) yields randomly correlated wind* and density profiles

Parameter Area	Parameters Varied
RCS Tanks	Oxidizer and fuel loaded in the tanks (by tank)
RCS Thrusters	Thrust, specific impulse, and mixture ratio
Boost Separation Motors and Ullage Motors (propellant settling motors for J-2X start)	Mounting errors (includes effect of uncertainty in the desired pointing direction), burn rate
Mass Properties	SRB inert mass, Upper Stage dry mass, interstage mass, Launch Abort System mass, Service Module/Crew Module/Spacecraft Adapter mass
Navigation	Initial position, velocity, and attitude errors for each direction; accelerometer bias, scale factor, and noise for each axis; gyro bias and scale factor for each axis

* Includes wind gusts but not small scale, very intense gusts.

Design Variations versus Flight Day Uncertainties

Monte Carlo dispersion simulations are intended to represent the variations that are possible when the vehicle flies. That is, on flight day, after the J-2X has already been hot-fired and measured, the first stage temperature is approximately known, and the various elements have been weighed, how much unknown variation may there be? How much extra fuel needs to be carried to ensure the vehicle reaches orbit? How much will the loads, etc. vary? On the other hand, at this early stage in design, there is design uncertainty regarding each of the vehicle parameters being varied. Each J-2X engine will have a different thrust, specific impulse, and mixture ratio as measured on the test stand. So how should the flight day unknowns and the flight day knowns (but variations between vehicles nonetheless) be balanced? In the set of dispersion results shown in this paper, these two uncertainty sources were lumped together. In subsequent dispersion simulations, they will be separated. In particular, a "heavy/slow" and "light/fast" vehicle will be chosen to represent the unknowns in vehicle design, and the expected flight day uncertainty will be used to conduct the Monte Carlo simulations for each of these vehicles.

Dispersion Simulation Groundrules

This section describes some groundrules and adjustments made to support the generation of the necessary results.

Unusable liquid oxygen and liquid hydrogen are consumed in simulation, when needed in low-performing dispersed trajectories, to ensure that all dispersed simulations reach orbit. This facilitates calculation of orbit injection error statistics and required Flight Performance Reserve without impacting the vehicle dynamics during ascent (except for a small effect on slosh dynamics at the very end of flight for a few cases that use the unusable propellant). Shutdown based on fuel depletion severely skews the statistics for orbit injection error and makes determination of FPR more difficult. As the vehicle design matures and the Flight Performance Reserve stabilizes to the appropriate amount, this artificial modeling will not be needed.

Inputs are dispersed randomly without clipping the inputs at a 3-sigma value. A maximum value for each input may be set if it is unreasonable for this input to ever exceed that value. Customers will decide individually whether or not to cut off certain output results that fall in the distribution tails, based on need. For example, if a 3 sigma value of propellant or max Q is desired, trajectories that fall outside these regions would be deleted or ignored.

The value of the 3 sigma output will be calculated as $1.5 \times$ the statistical 2 sigma level. This method will reduce the error involved in using the data points in the sparsely populated tail of the distribution (as compared to finding a 3 sigma value by looking at the data points near the 99.865% point). Taking 3×1 -sigma is an option, but if the distribution is not Normal, there could be significant error.

Figure 9 shows the results from comparing various numbers of Monte Carlo simulations to a run of 20,000 simulations. These data can be used in determining what number of runs is necessary. For a number of output parameters of interest, the percent variation in sigma level between that number of runs

and the sigma level from 20,000 runs was recorded. The figure shows the average of these variations. While the average smoothly decreases with larger numbers of runs, the value of each parameter is not as well behaved and depends on the random nature of the input dispersion cases. In a run of 20,000 runs performed, there are 20 sets of 1,000 runs. So the worst dataset and best dataset are the deviations in the sigma levels from the set of 1,000 runs that varied the most and from the set that varied the least, respectively.

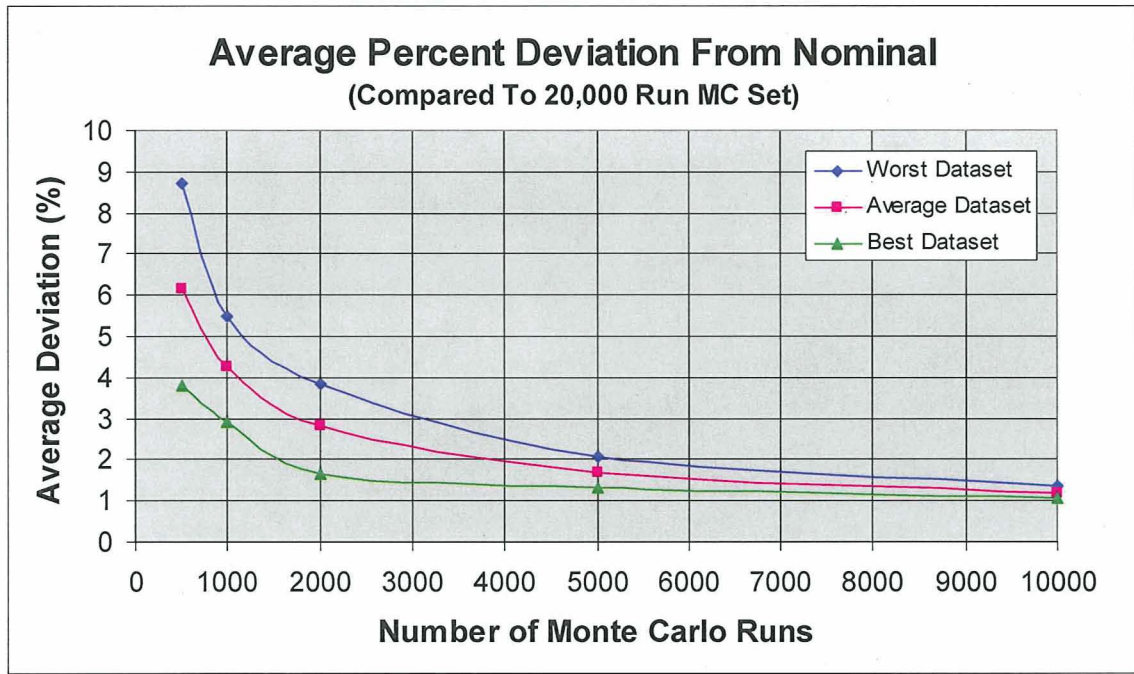


Figure 9: Comparison of Number of Monte Carlo Simulations

Each Monte Carlo result will consist of 2000 runs based on the results of Figure 9, with the need for a reasonable computer runtime included. This number of runs should be large enough to produce stable output without overwhelming the computing capability available as the model fidelity increases.

Monthly Comparisons

In order to determine which cases to concentrate on for the future, three degree-of-freedom (3DOF) Monte Carlo runs were made for each month and for both the ISS and lunar missions. For each case, the reference trajectory (and therefore open-loop guidance profile for first stage flight) was optimized using the mean monthly wind for that month and the average SRB Propellant Mean Bulk Temperature (PMBT) for that month. Data were generated that compared all months (examples are in Figures 10-14). The ISS engine thrust was lower for these cases compared to the current value (same for both missions), so comparing ISS to exploration results may lead to false conclusions. But they do show the monthly trends. For all the parameters that correlate with launch month, the worst months are February, July, or August.

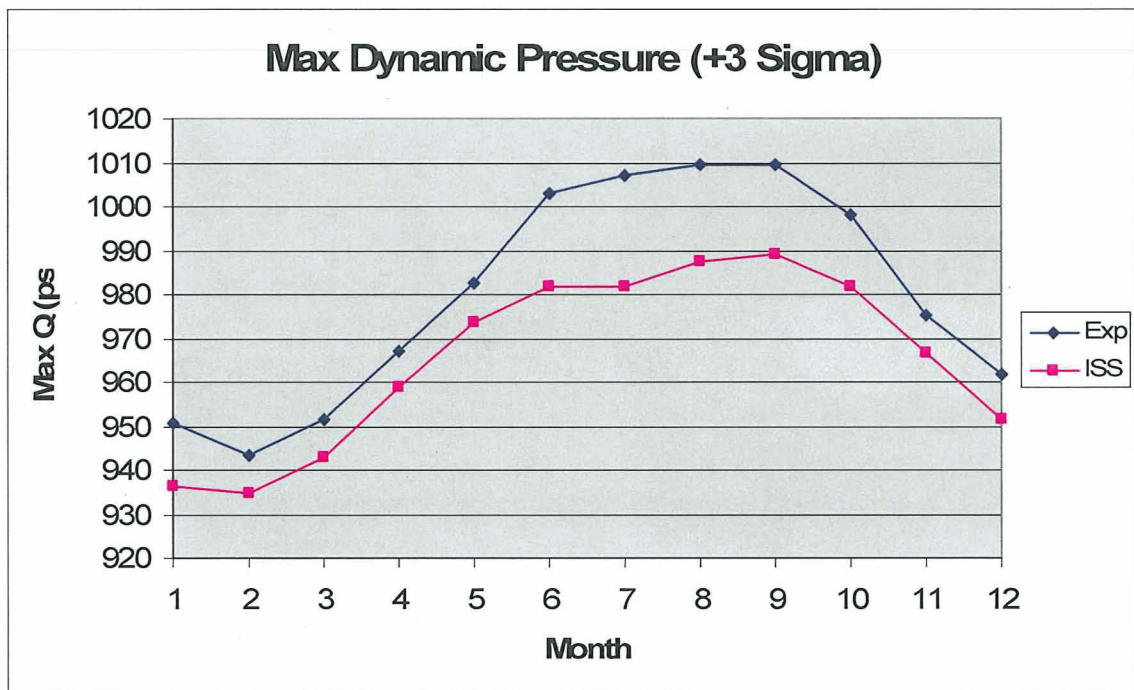


Figure 10: Maximum Dynamic Pressure comparison for all months

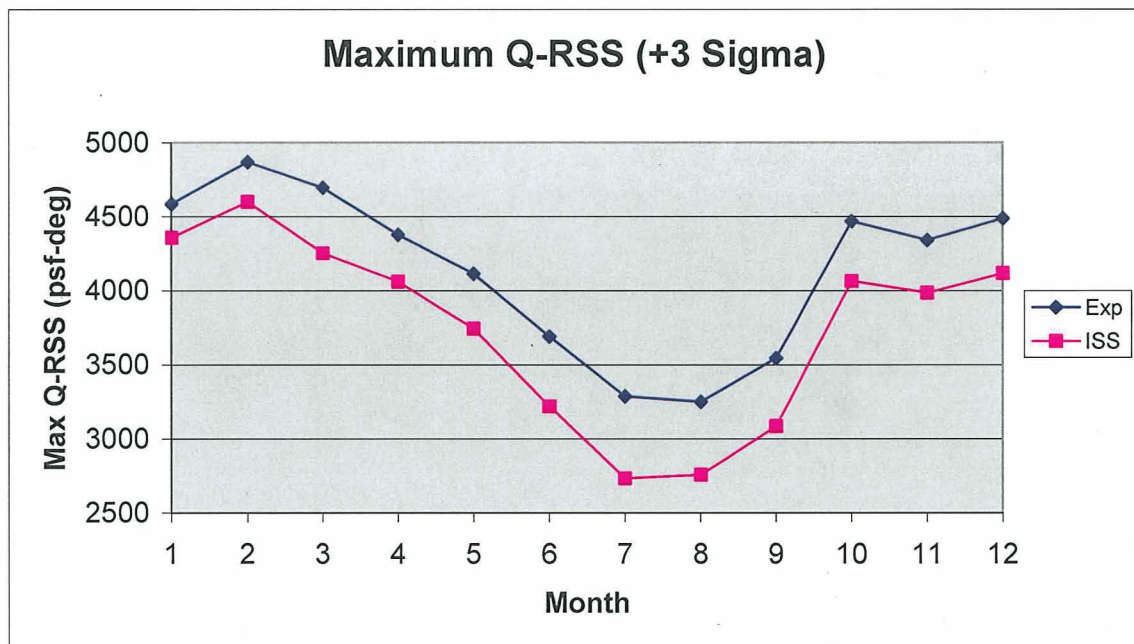


Figure 11: Maximum Dynamic Pressure times composite aerodynamic angle comparison for all months.

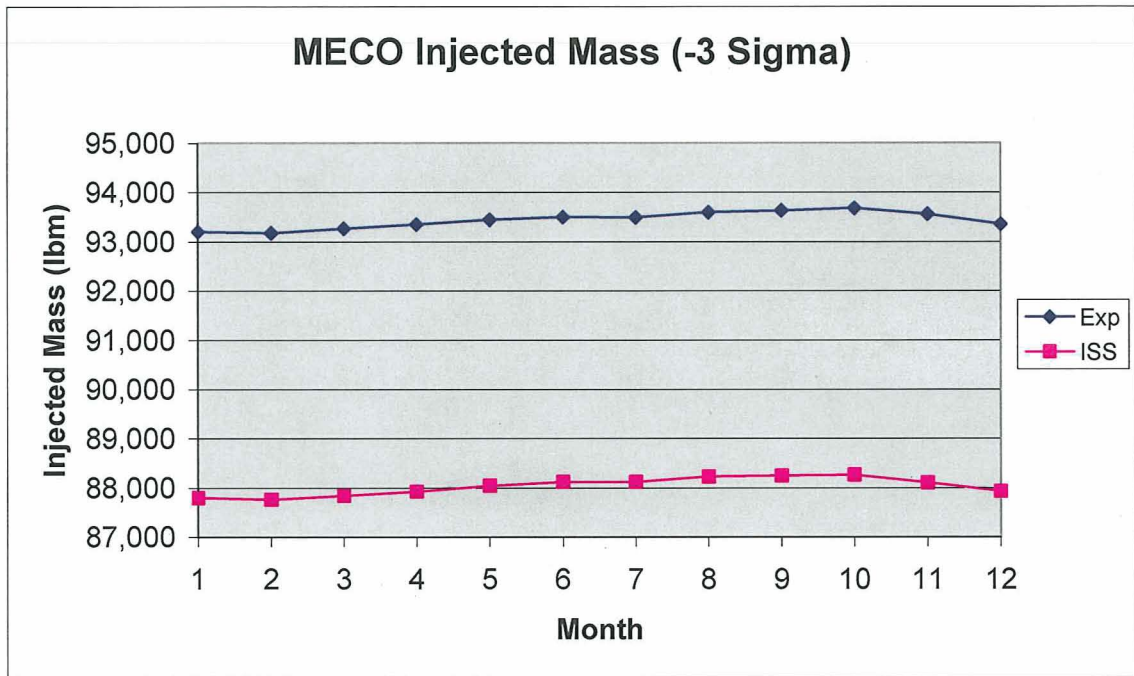


Figure 12: Injected mass comparison for all months

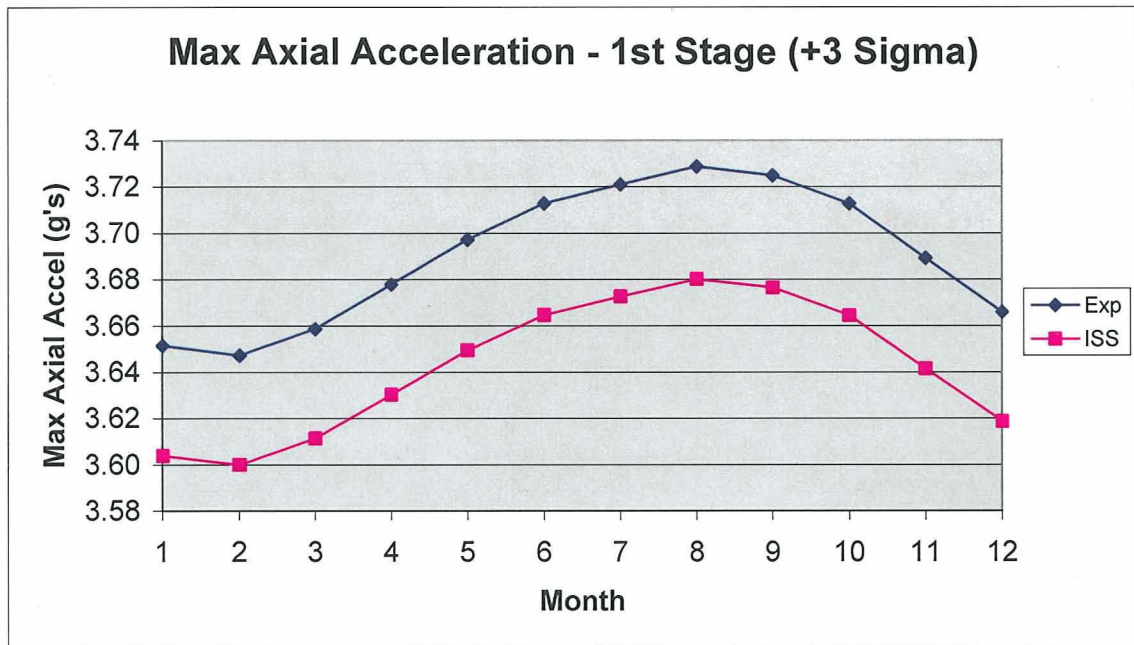


Figure 13: Maximum axial acceleration comparison for all months. Axial acceleration is higher in first stage than in second stage.

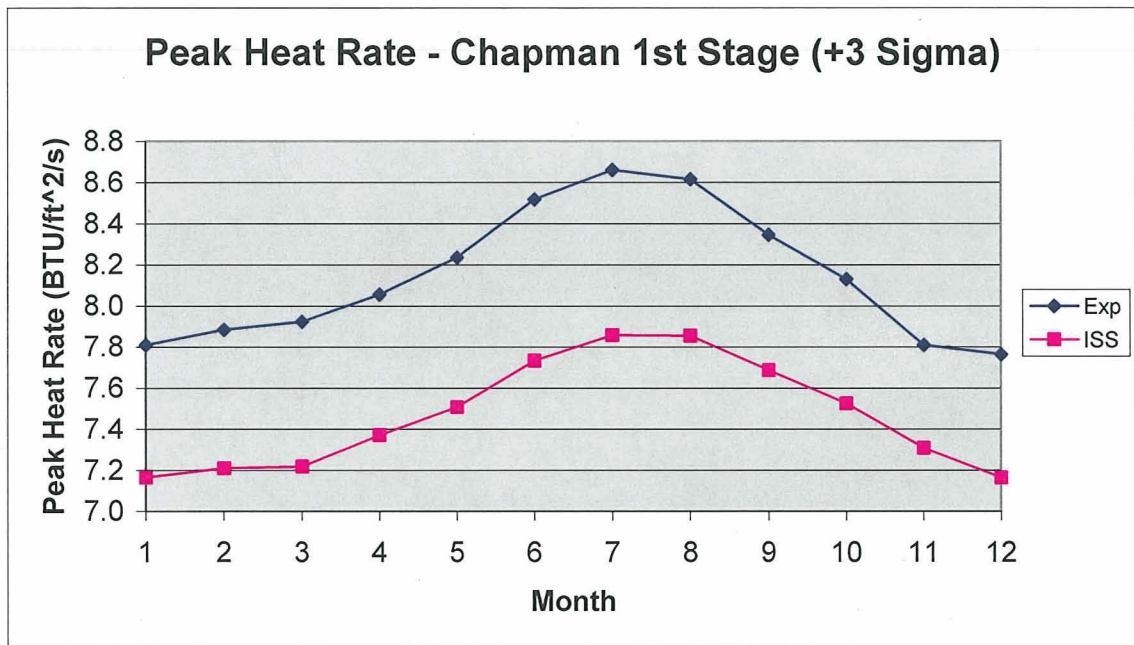


Figure 14: Peak heat rate comparison for all months. First stage heating drives much of the system.

Missions/Vehicle Models to Run

Now that the monthly data are available, which cases need to be run? That is, which cases, if run, lead to generation of the worst case results for the various disciplines? Besides having two missions and 12 possible months, there is the heavy/slow and light/fast vehicle models mentioned earlier, as well as a determination of whether the time point chosen to launch within a launch window should be at the beginning, nominal time, or end of the window. Clearly the curse of dimensionality ensures problems if the number of cases are not reduced. Using the data in the previous figures for the monthly variations along with engineering knowledge for the various disciplines leads to Table 12.

Table 13: Required Monte Carlo Runs. Q is dynamic pressure. RSS is root sum square. 3DOF is three degrees of freedom. 6DOF is six degrees of freedom. US is Upper Stage. SM is Service Module. RCS is reaction control system. TVC is thrust vector control. FPR is Flight Performance Reserve.

Mission	Month	H/S-L/F	Launch Window	Parameter	Comments/runs needed
Expl	February	L/F	Close	Q*RSS aero angle; acceleration angles; early aborts	3DOF and 6DOF
ISS	August	L/F	Open	Max Q, max axial accel; first stage heating indicator; max drag; early aborts; Upper Stage and 1 st stage footprint; effect of offloaded SM for late aborts; US re-entry aerothermal (TBR), RCS (roll maneuver)	3DOF and 6DOF
Expl	February	H/S	Close	Lunar performance/FPR*; Upper Stage and 1 st stage footprint	2 cases; 3 sigma high/low MR; 3DOF and 6DOF
Expl	February	H/S	Open	Upper Stage and 1 st stage footprint	3DOF

Mission	Month	H/S- L/F	Launch Window	Parameter	Comments/runs needed
ISS	February	H/S	Open	TVC (gimbal angles), ISS performance/FPR*	2 cases; 3 sigma high/low MR; 3DOF and 6DOF
ISS	August	L/F	Close	Upper Stage and 1 st stage footprint	3DOF

* Some summer months may have slightly less propellant remaining (for example, August Exploration had 7 lbm less LOX than February in the last set of dispersions), but February drives the performance

Most Recent 6 Degree of Freedom Dispersion Results

For the dispersion results shown below, the uncertainty inputs represent combined flight day and design uncertainties. These results are thus not broken out into heavy/slow and light/fast with flight day uncertainties as described above. This new breakout will occur for the next set of dispersion simulations. The vehicle model used for these runs was the nominal vehicle. There were four cases: the two missions and the months of February and August. Results are shown in the figures below, which display a sample of results from missions and months that were the most extreme. A very extensive set of data was derived from the dispersion simulations.

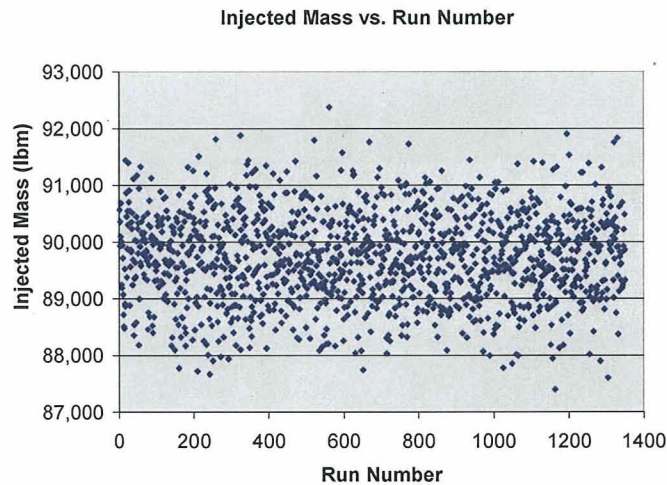


Figure 15: Injected Mass for ISS Mission, February

Max Heat Rate (Chapman) vs. Mach at Max Heat Rate

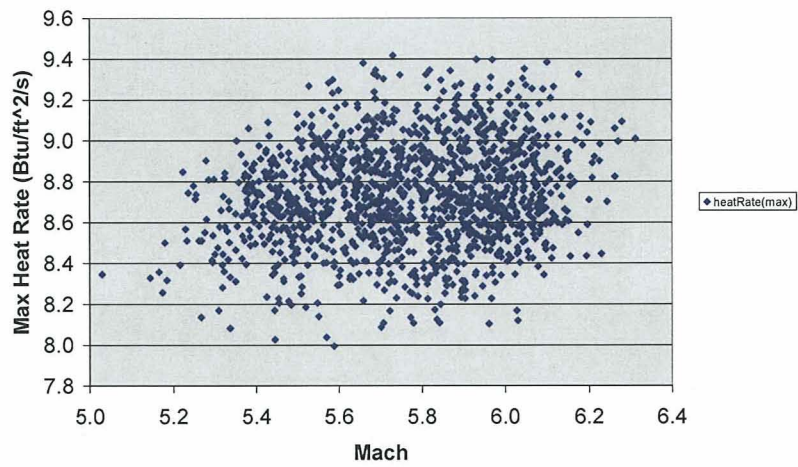


Figure 16: Peak Heat Rate for Lunar Mission, August

Injection Apogee vs. Perigee Altitudes

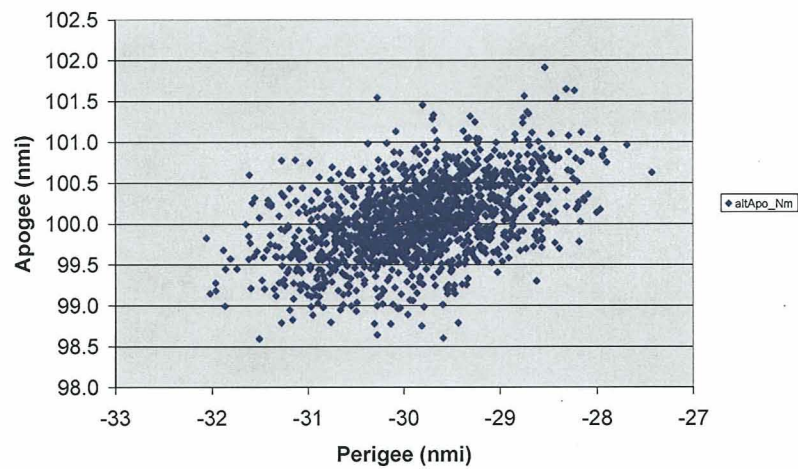


Figure 17: Injection Apogee vs Perigee, Lunar Mission, August

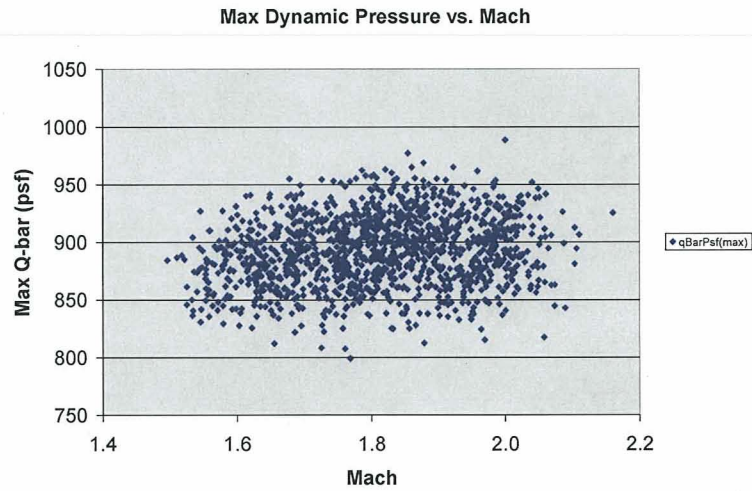


Figure 18: Maximum Dynamic Pressure, Lunar Mission, August

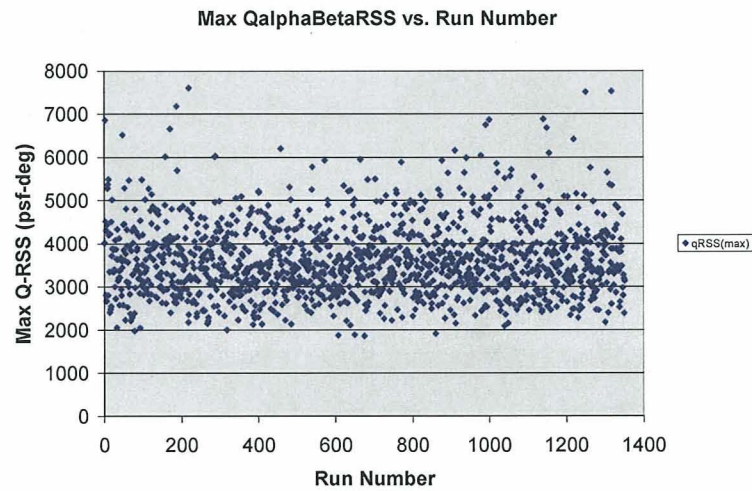


Figure 19: Maximum Dynamic Pressure times Aerodynamic Angle, Lunar Mission, February. This is a structural bending indicator. The size of these results is partly related to the use of monthly mean wind biasing (as opposed to day of launch wind biasing). It is also expected that the peak values will decrease when the control system is further refined (to track the guidance commands more tightly).

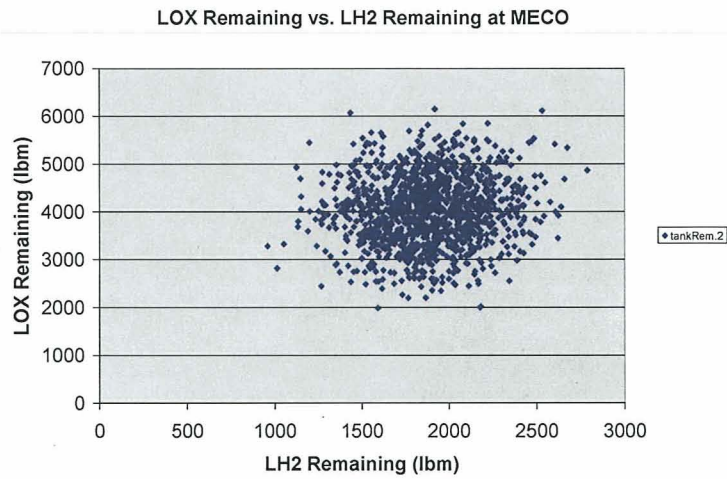


Figure 20: Propellant Remaining, ISS Mission, February. This variation leads to sizing of the Flight Performance Reserve in order to guarantee that all cases reach orbit.

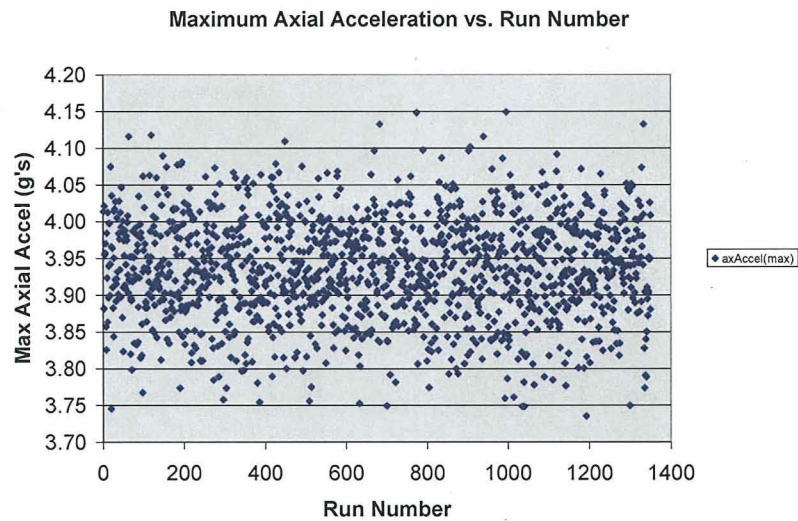


Figure 21: Maximum Axial Acceleration, Lunar Mission, August

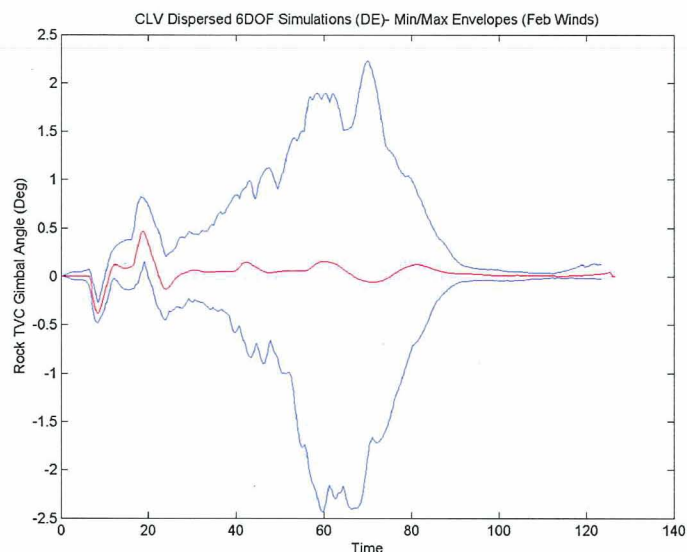


Figure 22: Gimbal Angle Envelope with Mean Shown. Lunar Mission, February

CONCLUSION

Use of Monte Carlo simulation is a powerful tool for launch vehicle design, and is providing critical data to the various design disciplines for Ares-I and for the Orion spacecraft. This paper shows the current status of this work. The set of results is much more extensive than what would fit in a technical paper. There is much more to be done as the design matures.

REFERENCES

Add trajectory references here

Renyou Wang and Urmila Diwekar, "Latin Hypercube Hammersley Sequence (LHHS) – Reverse Radix Leaped (RR2L) Sampling Technique", Department of Engineering & Public Policy, Carnegie Mellon University,
http://custom.ce.cmu.edu/archives/12162001/miniconference/cdrom/POSTERFILES/RENYOU_WANG_2.pdf

Robinson, D. and Atcitty, C., "Comparison of Quasi- and Pseudo- Monte Carlo Sampling for Reliability and Uncertainty Analysis," paper AIAA 99-1589.

Gregory D. Wyss and Kelly H. Jorgensen, "A User's Guide to LHS: Sandia's Latin Hypercube Sampling Software", Sandia National Laboratories, SAND98-0210, 1998.

"The Halton Sequence," Iowa State University,
http://www.math.iastate.edu/reu/2001/voronoi/halton_sequence.html, 2001.

Wong, T.T., Luk, W. S., and Heng, P.A., "Sampling with Hammersley and Halton Points",
<http://www.cse.cuhk.edu.hk/~ttwong/papers/udpoint/udpoint.pdf>

Justus, C.G., and D.L. Johnson, "The NASA/MSFC Global Reference Atmospheric Model -1999 Version (GRAM-99)", NASA/TM--1999-209630, 1999.